Effect of the network density on dynamics of the soft and the Goldstone modes in short-pitch ferroelectric liquid crystals stabilized by an anisotropic polymer network

Mohamed Petit, Jamal Hemine, and Abdelylah Daoudi
Laboratoire de Thermophysique de la Matière Condensée-Equipe de l' UMR-CNRS 8024, Université du Littoral Côte d'Opale, 145, Avenue Maurice Schumann, 59140 Dunkerque, France

Mimoun Ismaili and Jean Marc Buisine
Laboratoire de Dynamique et Structure des Matériaux Moléculaires, UMR-CNRS 8024, Université des Sciences et Technologies de Lille, Batiment P5, 59655 Villeneuve d'Ascq Cedex, France

Antonio Da Costa
Laboratoire de Physico-Chimie des Interfaces et Applications (LPCIA), FRE-CNRS 2485, Faculté des Sciences Jean Perrin, Université d'Artois, Rue Jean Souvraz, SP 18, F-62307 Lens, France
(Received 9 October 2007; revised manuscript received 27 June 2008; published 30 March 2009)

We report the influence of the polymer network density formed in short-pitch ferroelectric liquid crystal (FLC) on the soft and the Goldstone dielectric relaxation modes. The experimental results of the pure FLC and the FLC stabilized by a polymer network with various densities are presented and compared. These results reveal that in the SmC^* phase, when the polymer concentration increases, the Goldstone dielectric strength gradually decreases and the relaxation frequency is shifted to higher values. In the SmA^* phase, the results show that close to the SmC^*-SmA^* transition temperature, T_c, the soft relaxation mode is largely influenced by the polymer network: a sharp decrease in the dielectric strength and an increase in the relaxation frequency when the polymer density increases were observed. The soft mode is relatively weakly affected by the network for higher temperatures ($T \geq T_c + 0.5$ °C). This indicates that the behavior of the soft mode for this temperature domain is dominated rather by thermal effects than by the network. A simple phenomenological approach was proposed to explain the behavior of the soft-mode dielectric strength versus polymer concentration. This model takes into account the anisotropic interaction between the polymer network and the liquid crystal, and the elastic interaction resulting from the anchoring of the liquid crystal molecules at the polymer surfaces. The experimental results are in agreement with the proposed model.

DOI: 10.1103/PhysRevE.79.031705 PACS number(s): 61.30.Hn, 77.84.Nh

I. INTRODUCTION

During the previous decades, the study of ferroelectric liquid crystals (FLC) in confined geometry has been an active area of research. Understanding of the smectic layer structure, dynamics of collective modes, and molecular motions can be advanced if results on samples restricted to confined geometries are compared with those of the bulk.

Generally, spatially confined FLC exhibit a drastically reduced Goldstone mode: a considerable decrease in the dielectric strength being observed [1–9] along with the relaxation frequencies shifted to higher values [5]. These effects were explained by the increase in the effective elastic energy [5] of the materials. The behavior of the soft relaxation mode is however still not sufficiently described in the literature. Most of these studies concerned systems with FLC confined in nanoporous membranes with separated cylindrical pores [10], porous glasses with narrow pore size distributions [11], or silica aerogels with irregularly shaped cavities and broad size distributions [5]. To gain better understanding of the dielectric properties of the confined FLC, different topologies, such as a network of straight rods or anisotropic polymer bundles dispersed in the FLC media, may be studied.

Polymer-stabilized liquid crystals (PSLCs) are composite materials in which a small concentration of the polymer network is dispersed within liquid crystal media [12,13]. The possibility to stabilize liquid crystal cells by a polymer network was first demonstrated by Hikmet [14]. The polymer network is formed by a chemical cross-linking process of a small concentration (few percent) of photoreactive monomers dissolved in low molecular weight mesogenic material and activated by a UV illumination. When the polymerization occurs in an aligned geometry, the resulting polymer network is roughly aligned parallel to the direction initially imposed by the liquid crystal medium in which the network has been formed [15,16]. In turn, the alignment of the liquid crystal can be reinforced by the polymer fibrils through a bulk anchoring mechanism due to a large quantity of small internal boundaries. Depending on the type of the reactive mesogen, the morphology of the polymer network may correspond to an open structure consisting of anisotropic and interconnected fibrils [15,17–20]. The lateral size of the fibrils is of the order of a few tenths of 1 μm [21–23]; their density increases with the reactive monomer concentration. The polymer morphology also depends on the nature of the liquid crystal phase in which the network was formed. In fact, previous studies have shown that the polymer fibers adopt a characteristic helically twisted form, taking place spontaneously during the photocuring process in the cholesteric [16,19–21,24–28] and in the chiral smectic phases [29].

The electro-optic properties of liquid crystals can be modified by the presence of the polymer network [13]. Ap-

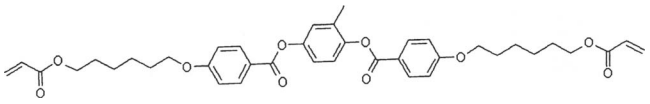

FIG. 1. The molecular structure of the reactive monomer.

plication of an electric field causes a distortion of the liquid crystal host due to a field-induced director rotation without any reorientation of the network [15], considered to be rigid and heavily cross linked. However, the polymer network imposes additional alignment forces on the liquid crystal molecules supporting the initial orientation of the liquid crystal media prior to the photopolymerization process [14,30,31]. The electro-optical response of such systems is characterized by a critical field for director reorientation and fast response dynamics [15,18,32,33].

In a recent study [29], we have demonstrated that when the polymer network is formed in the short-pitch ferroelectric liquid crystal, the critical field necessary to unwind the helical structure of the FLC increases with the polymer density. These results are interpreted by the increase in the apparent elasticity of the polymer-stabilized ferroelectric liquid crystal (PSFLC) films resulting from the twist morphology of the polymer fibers. The electroclinic susceptibility as well as the electroclinic switching time has been shown to be largely influenced by the polymer network [34,35]. This behavior was explained by a strong interaction between the liquid crystal molecules and the polymer network [34,35].

In the present contribution, we show how the introduction of a small quantity of an anisotropic polymer network formed in a short-pitch SmC^* phase affects the dynamics of the ferroelectric relaxation mechanisms. After describing the experimental observations, we demonstrate that the changes in the dielectric behaviors of the PSFLC might be explained mainly by the increase in the elasticity of the films. In addition, a theoretical analysis based on an extended phenomenological model is proposed and discussed in order to show how the confining polymer network influences the relaxation behavior in the orthogonal smectic *A* phase.

II. EXPERIMENTS

The ferroelectric liquid crystal compound used in this work is the ROLIC 8823 (Rolic Research Ltd.) which exhibits, on heating, the following phase sequence between the crystalline (Cr) and the isotropic liquid (*I*) phases: Cr-27 °C-SmC^*-63.5 °C-SmA^*-65 °C-*I*, where SmC^* and SmA^* are the chiral smectic-*C* and smectic-*A* phases, respectively. In the SmC^* phase the helical pitch at room temperature is about 0.3 μm and the spontaneous polarization is $P_s \approx 100$ nC/cm^2. The polymer network is prepared using a reactive diacylate mesogen as a photocurable monomer which exhibits the nematic (*N*) phase between Cr and *I* phases (Cr-88 °C-*N*-118 °C-*I*). The molecular structure of this monomer is shown in Fig. 1. The photopolymerization was initiated with Irgacures 369 which was added to the monomer with a concentration of 0.5 wt %. The reactive monomer, together with photoinitiator, was dissolved into the ferroelectric liquid crystal in its isotropic phase to make a homogeneous mixture. The monomer concentration in the mixture was varied between 2 and 7 wt %. A 5-μm-thick cell with polyimide aligning layers (EHC Inc., Japan) with polyimide aligning layers was filled with a mixture in its isotropic phase. In order to obtain a good alignment of smectic layers, an electric field of 5 V μm^{-1} at 1 Hz was applied to cells, and they were slowly cooled at 0.1 °C min^{-1} from the isotropic phase down to room temperature. The sample cells were subsequently exposed to ultraviolet light (wavelength $\lambda = 365$ nm) at 25 °C with an intensity of 18 mW cm^{-2} for 30 min without any applied electric field.

Dielectric measurements were performed in the frequency range of 10 Hz–13 MHz (HP 4192A). In order to obtain the characteristic dielectric strengths and relaxation frequencies of the ferroelectric relaxation modes, the dielectric spectra were fitted simultaneously by the Cole-Cole function,

$$\epsilon^* = \epsilon_\infty + \frac{(\Delta\epsilon_G)}{1 + (jf/f_G)^{(1-\alpha_G)}} + \frac{(\Delta\epsilon_s)}{1 + (jf/f_s)^{(1-\alpha_s)}} + \frac{\sigma}{j2\pi f\epsilon_0}, \tag{1}$$

where f is the frequency, ϵ_∞ is the high-frequency limit of the dielectric permittivity, and $\Delta\epsilon_G$ and $\Delta\epsilon_s$ represent the dielectric strengths corresponding to Goldstone and soft modes, respectively. f_G and f_s represent the relaxation frequencies of the two modes, α_G and α_s are the distribution parameters, and σ is the electric conductivity. To image the topography of the polymer networks, a Veeco multimode atomic force microscopy (AFM) equipped with a Nanoscope IIIa controller was used. All AFM scans were taken in tapping mode with commercially available tips made of phosphorus-doped silicon.

III. RESULTS AND DISCUSSION

A. Goldstone mode in the SmC^* phase

Figures 2(a) and 2(b) show examples of the dispersion, $\epsilon'(f)$, and absorption, $\epsilon''(f)$, dielectric spectra obtained in the SmC^* phase at low temperatures for different polymer concentrations. For all of the concentrations studied, two relaxation mechanisms were detected. The first, at low frequencies (between 1 and 3 kHz) with a high amplitude, is due to the Goldstone mode; whereas the second observed at high frequencies ($\geq$1 MHz) with a weak amplitude is an artifact due to the indium tin oxide (ITO) conducting layers. As shown in Fig. 2(a), at low frequencies, the dielectric response shows a very strong polymer concentration dependence; at 100 Hz, for example, ϵ' decreases from 100 to 30 when the polymer concentration increases from 0% to 7%. This effect is also clearly illustrated in the behavior of the absorption peak observed in the ϵ'' spectra [Fig. 2(b)]; the absorption peak strongly decreases from 48 to 8 when the polymer concentration is varied from 0% to 7%. The parameters $\Delta\epsilon_G$ and f_G obtained from the curve-fit procedure are displayed in Figs. 3(a) and 3(b). The behavior of $\Delta\epsilon_G$ versus temperature showed the same general features for all the samples [Fig. 3(a)]; $\Delta\epsilon_G$ slightly increases to reach a maximum at a temperature called T_{max} (3 °C below T_c) then decreases abruptly above T_{max}. The behavior of $\Delta\epsilon_G$ versus temperature is de-

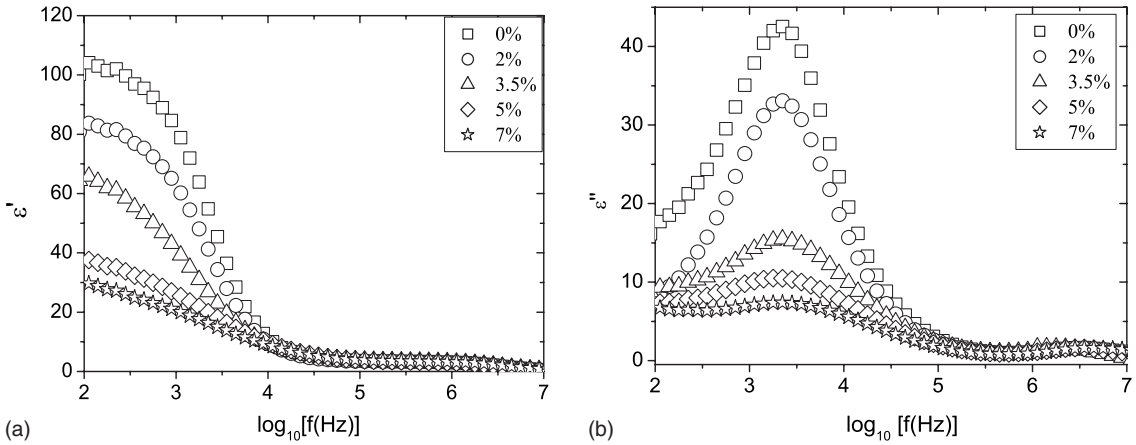

FIG. 2. Frequency dependence of (a) the real and (b) the imaginary parts of complex permittivity in the smectic C^* phase for different polymer concentrations at $T=25$ °C.

pendent on that of the helical pitch of the FLC (Fig. 4). Usually the maximum observed in $\Delta\epsilon_G(T)$ is related to that exhibited by the helical pitch (Fig. 4) at temperatures close to T_c and indicates that the helical structure of the FLC is preserved in all our PSFLC systems. This behavior is in accordance with the results reported in [29], which demonstrate that the helical structure of the ferroelectric phase still exists despite the presence of the polymer network. The temperature dependence of the Goldstone relaxation frequency [Fig. 3(b)] shows that f_G slightly increases with temperature, reaches a maximum, and then rapidly decreases to a minimum value at a temperature corresponding to T_{max} [Fig. 3(b)]. After T_{max}, an abrupt increase in f_G is observed for a temperature close to T_c. Qualitatively, the thermal behavior of the Goldstone mode is not affected by the polymer network. However, quantitative differences were observed for $\Delta\epsilon_G$ and f_G when the polymer network density increases. To illustrate this effect, we present on Figs. 5(a) and 5(b) the evolution at room temperature of $\Delta\epsilon_G$ and f_G as a function of the polymer concentration. It can be seen from these figures that the increase in the polymer concentration from 0% to 7% leads to a breakdown of $\Delta\epsilon_G$ from 120 to 27 and to an increase in f_G from 1.5 to 3.5 kHz. Changes in the dynamic of the Goldstone mode have already been observed in PS-FLC systems by Gasser *et al.* [1] and in other composite-based FLC, as a random network formed from dispersions of aerosil particles within FLC media [6–8]. For aerosil/FLC composites, a decrease in $\Delta\epsilon_G$ [6–8] and a shift of f_G toward high frequencies [7,8] with increasing the density of aerosil particles were observed. The Goldstone mode even disappears in these systems for a sufficiently high aerosil density. The authors have interpreted the behavior of the dielectric response in these systems by size effects on smectic domains [6–8]; the reduction in the Goldstone mode strength and the increase in the relaxation frequency with increasing the concentration of aerosil particles are due, according to these authors, to the formation of smaller smectic domains where fluctuations are quenched by surface interactions, leading to a deformation of the helix. Additionally, the orientation of these smectic domains becomes randomly distributed so that fewer domains are therefore preferentially oriented in the direction of the applied electric field. We believe that the interpretation given above cannot explain the behavior of our PSFLC systems, despite similar changes in dielectric relaxation being observed. First, the polymer network in PSFLC cells are anisotropic and stabilizes the configuration of smec-

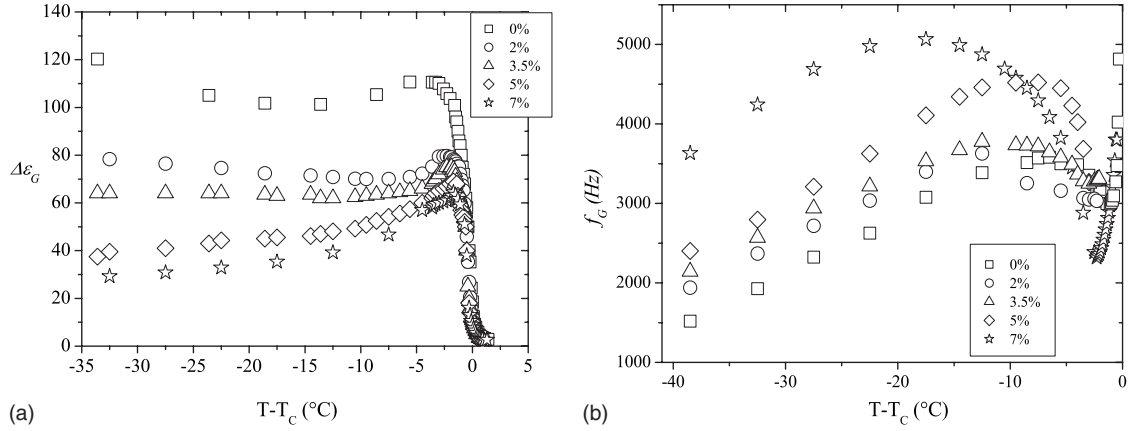

FIG. 3. Temperature dependence of (a) the dielectric strength and (b) the relaxation frequency of the Goldstone mode for different polymer concentrations.

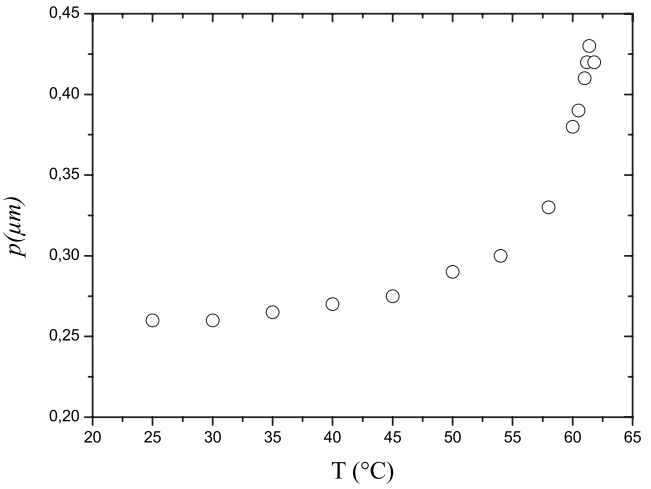

FIG. 4. Temperature dependence of the helical pitch of the pure FLC measured by mean of Grandjean-Cano method [37].

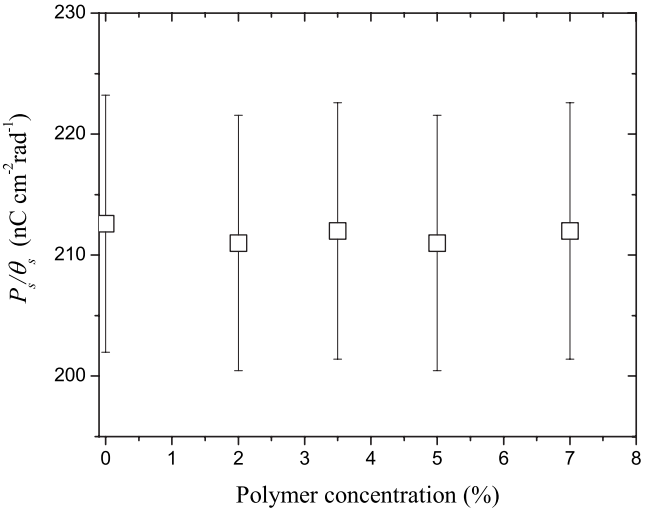

FIG. 6. P_s/θ_s ratio measured at $T=25$ °C versus polymer concentration.

tic domains oriented preferentially to the direction of the electric field. Second, we have previously demonstrated [29] that the polymer network in our systems presents a fibrillar structure with a twisted morphology. This morphology prevents the deformation and the unwinding of the helical structure of the SmC^* phase. Accordingly, we think that the changes observed in dielectric response in our systems are essentially governed by elastic effects. We have already interpreted the distortion of the helical structure of the SmC^* phase in terms of an elastic coupling between the polymer network and the FLC molecules due to the anchoring forces at the polymer fiber surfaces [29]. We expect that the network-FLC interactions enhance the apparent elasticity of the PSFLC films, and accordingly, causes the increase in the relaxation frequency f_G and the reduction in dielectric strength $\Delta\epsilon_G$. In fact, the dielectric strength and the relaxation frequency of the Goldstone mode are expressed as [36]

$$\Delta\epsilon_G = \frac{1}{2\epsilon_0 K_{\text{eff}} q_0^2}(P_s/\theta_s)^2, \tag{2}$$

$$f_G = \frac{K_{\text{eff}} q_0^2}{2\pi\gamma_{\text{eff}}}. \tag{3}$$

If we assume the these expressions remain valid for our PSFLC systems, then K_{eff} and γ_{eff} denote the effective twist elastic constant and the Goldstone rotational viscosity of the PSFLC films, respectively. θ_s and P_s are the tilt angle and the spontaneous polarization, respectively. $q_0=\frac{2\pi}{p}$, where p is the helical pitch of the FLC that is considered here to be constant. The reduction in $\Delta\epsilon_G$ as a function of polymer concentration is attributed to the variation in $\frac{P_s}{\theta_s}$ and/or K_{eff}. To clarify that, we have plotted in Fig. 6 the ratio $\frac{P_s}{\theta_s}$ as a func-

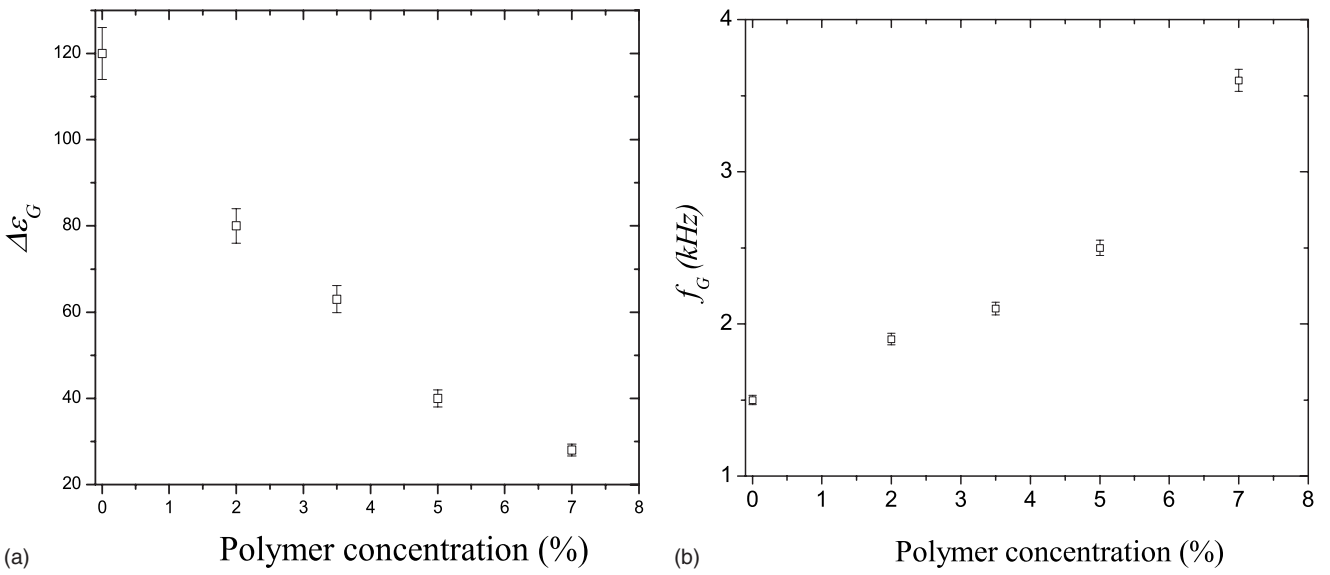

FIG. 5. (a) $\Delta\epsilon_G$ and (b) f_G measured at $T=25$ °C versus polymer concentration.

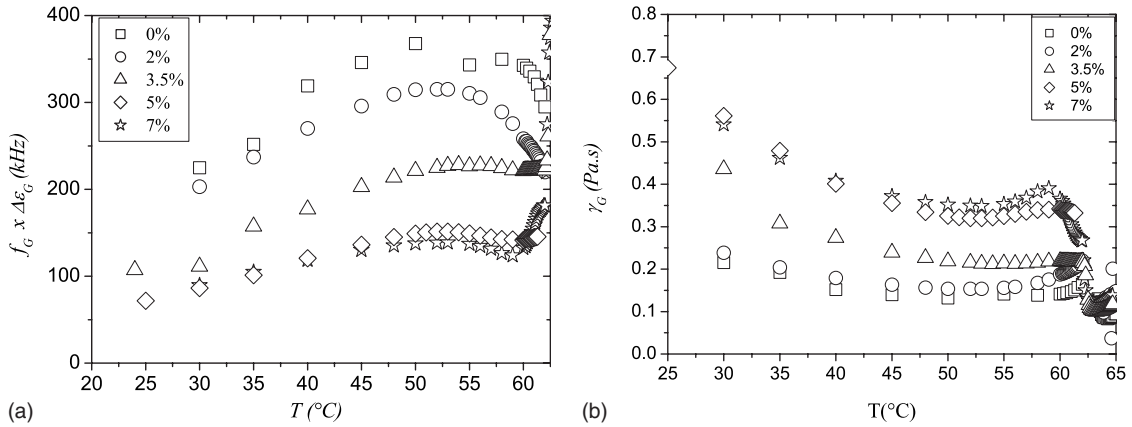

FIG. 7. Temperature dependence (a) of $\Delta\epsilon_G \times f_G$ and (b) of the rotational viscosity γ_{eff} of the Goldstone mode for different polymer concentrations.

tion of polymer concentration. This figure shows that this ratio can be considered independent of the polymer concentration. As a consequence, the observed decrease in the $\Delta\epsilon_G$ with polymer concentration can be explained rather by the increase in the effective elastic constant K_{eff}. On the other hand, the relaxation frequency of the Goldstone mode [Eq. (3)] is controlled both by the elastic ($K_{\text{eff}}q_0^2$) and viscous (γ_{eff}) forces. The increase in f_G with polymer concentration can be explained by the decrease in the Goldstone rotational viscosity γ_{eff} and/or the increase in the effective elastic constant K_{eff}. From Eqs. (2) and (3), the effective rotational viscosity can be expressed as $\gamma_{\text{eff}} = \frac{(P_s/\theta_s)^2}{4\pi\epsilon_0\Delta\epsilon_G f_G}$. According to this expression and using the experimental data of $\Delta\epsilon_G \times f_G$ [Fig. 7(a)] and $\frac{P_s}{\theta_s}$ (Fig. 6), γ_{eff} was evaluated as a function of temperature for all polymer concentrations studied. Generally, γ_{eff} of the PSFLC films increases with the polymer network density. At room temperature, for example, γ_{eff} increases from 0.2 to 0.6 Pa s when the polymer concentration increases from 0% to 7% [Fig. 7(b)]. Consequently, the increase in the relaxation frequency with the network density is certainly due to the increase in the effective elastic constant K_{eff} [Eq. (3)]. To illustrate this, K_{eff} was evaluated at room temperature from Eqs. (2) and (3); the results are displayed in Fig. 8. This figure shows that K_{eff} linearly increases from 0.5×10^{-11} to 2.3×10^{-11} N when the polymer concentration increases from 0% to 7%. The values of K_{eff} found here compare well with those obtained for the same PSFLC systems from the electro-optic measurements [29]. In conclusion, the increase in the relaxation frequency and the reduction in the dielectric strength of the Goldstone mode for the PSFLC films seem to be due to the increase in the twist elastic energy, resulting from the strong interaction between liquid crystal molecules and the polymer network.

B. Soft mode in the SmA^* phase

Figures 9(a) and 9(b) show examples of the dispersion, $\epsilon'(f)$, and absorption, $\epsilon''(f)$, dielectric spectra obtained in the SmA^* phase at T_c for each polymer concentration. Two relaxation mechanisms are detected. The first, at frequencies between 10 and 30 kHz with a weak strength, is attributed to the soft-mode relaxation mechanism; whereas the second observed at high frequencies ($\geq$1 MHz) is due to the ITO conducting layers. As shown in Fig. 9(a), at 1 kHz frequency, the dielectric response shows a very strong polymer concentration dependence; ϵ' decreases from 23 to 12 when the polymer concentration increases from 0% to 7%. This effect is also clearly demonstrated from the behavior of the absorption peak observed in Fig. 9(b); the absorption peak decreases from 12 to 3 when the polymer concentration is varied from 0% t o 7%.

We present in Figs. 10(a) and 10(b) the temperature dependence of the dielectric strength, $\Delta\epsilon_s$, and the relaxation frequency, f_s, of the soft mode. For all studied concentrations, the behavior of $\Delta\epsilon_s$ versus temperature shows the same general features [Fig. 10(a)]. A rapid increase in $\Delta\epsilon_s$ is observed close to T_c for all concentrations studied. The increase in $\Delta\epsilon_s$ at and close to T_c is dependent on the polymer concentration [Fig. 10(a)]. Note that $\Delta\epsilon_s$ becomes relatively weakly affected by the network as temperature increases from T_c (Fig. 11). The relaxation frequency, f_s, exhibits a linear temperature dependence [Fig. 10(b)]. At T_c, f_s increases from 10 to 36 kHz when the polymer concentration

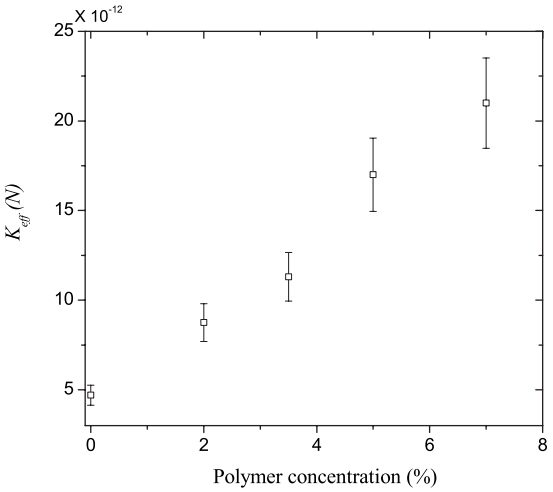

FIG. 8. The effective twist elastic constant K_{eff} versus polymer concentration.

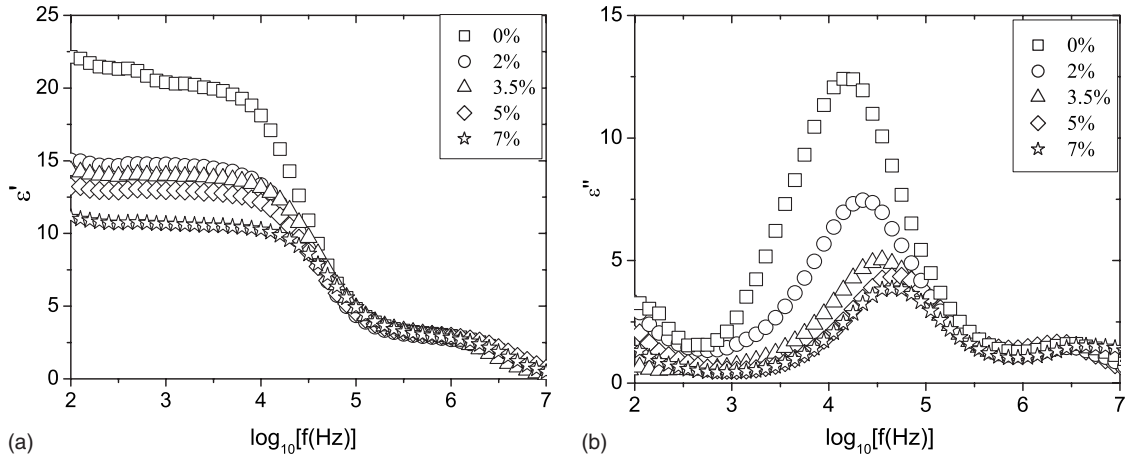

FIG. 9. Frequency dependence of (a) the real and (b) the imaginary parts of the complex permittivity at the SmC^*-SmA^* phase-transition temperature, T_c, for different polymer concentrations.

increases from 0% to 7%. This effect seems to be less dependent on the polymer network density at relatively higher temperatures ($T \geq T_c + 0.5\ ^\circ\mathrm{C}$) [Fig. 10(b)]. Similar behaviors have been observed in the case of dispersed silica particles on FLC matrix near the SmA^*-SmC^* phase transition [6–8]. However, Kundu *et al.* [38] showed for other PSFLC systems that the soft-mode dielectric strength remains unchanged when the FLC cells are stabilized by a polymer network formed from a nonmesogenic reactive monomer. These authors did not provide any indications of the network structure of their systems. However Beckel *et al.* [39] demonstrated that nonmesogenic monomers give rise to polymer chains which microseparate from FLC molecules in the smectic layers leading to a layer swelling. Obviously, this polymer network structure is completely different to that obtained in our systems (Fig. 12). In order to examine how the polymer network influences the soft-mode dielectric strength of the PSFLC, we used the model previously developed [34] to explain the electroclinic behavior of PSFLC films. We point out hereafter only on the principal results of this model.

The total free-energy density was expressed as

$$f_t = f_0 + \frac{1}{2}\alpha(T - T_0)\theta^2 - CP\theta + \frac{P^2}{2\epsilon_0\chi} - PE + \frac{1}{2}W_p\theta^2 + \frac{1}{2}K_2\left(\frac{\partial\theta}{\partial z}\right)^2, \tag{4}$$

where the f_0 term represents contribution of the undistorted SmA^* phase to the total free-energy density, α is the mean-field coefficient, C is related to the piezoelectric coupling between the field-induced polarization P_{ind} and the induced electroclinic tilt θ_{ind}, ϵ_0 is the vacuum permittivity, and χ is the dielectric susceptibility. K_2 is the twist elastic constant and W_p is the coupling coefficient describing the interaction between the polymer network and the liquid crystal molecular director. By minimizing f_t, the equilibrium of the system is obtained [34] for the average values,

$$\langle \theta_{\mathrm{ind}}^{\mathrm{PSFLC}} \rangle = \frac{\epsilon_0\chi CE}{\alpha(T - T_c')}\left[1 - \frac{\tanh(L_c/2a)}{(L_c/2a)}\right], \tag{5}$$

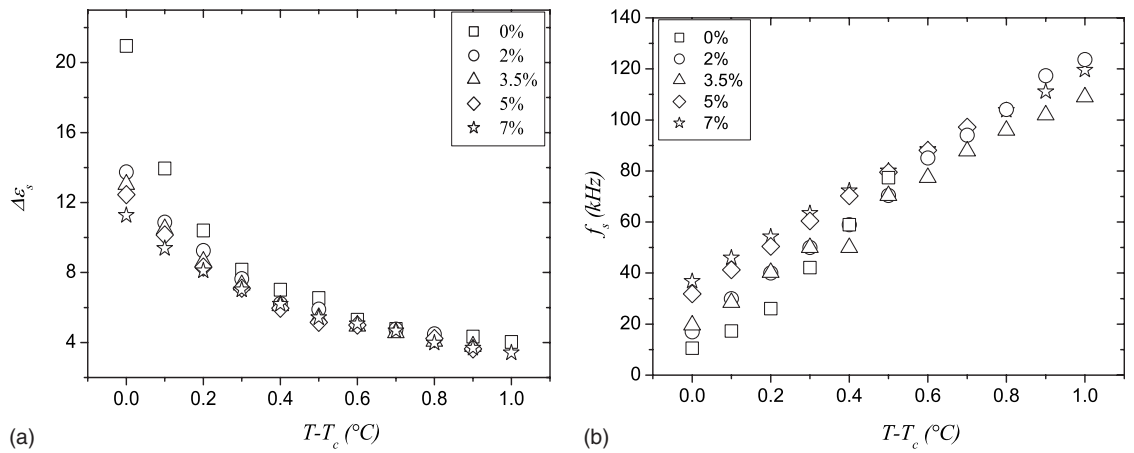

FIG. 10. Temperature dependence of (a) the dielectric strength $\Delta\epsilon_s$ and (b) the relaxation frequency f_s of the soft mode in the smectic A^* phase for different polymer concentrations.

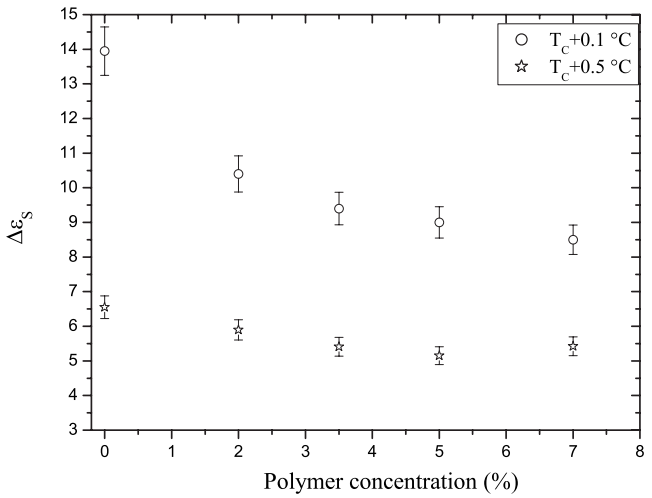

FIG. 11. The dielectric strength, $\Delta\epsilon_s$, of the soft relaxation mode versus polymer concentration.

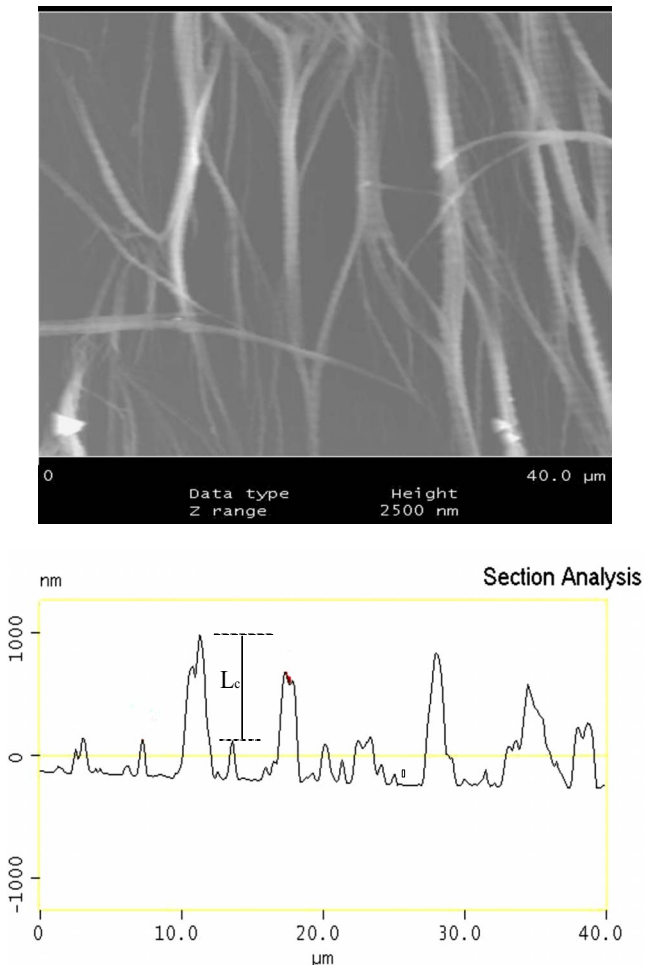

FIG. 12. (Color online) Tapping mode AFM images of the polymer network structure of 40×40 μm^2 (upper) and the height profile of the network structure (lower) of the 3.5% polymer concentration.

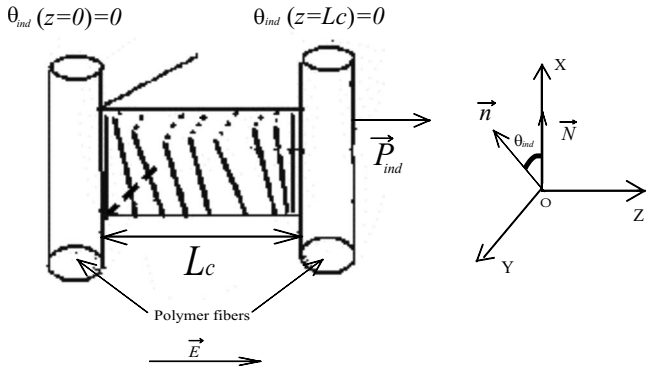

FIG. 13. Tilt angle, $\Theta_{\rm ind}$, and polarization $\vec{P}_{\rm ind}$, induced by the electric field $\vec{E}$ in the SmA^* layers confined between two successive fibers of the network. The elastic distortion of the liquid crystal director $\vec{n}$ is a twist deformation due to the anchorage of the liquid crystal molecules at the polymer fiber boundaries; $\vec{N}$ represents the polymer network director and L_c denotes the average distance between two successive polymer fibers in the direction of the applied electric field.

$$\langle P_{\rm ind}^{\rm PSFLC}\rangle = \epsilon_0\chi E + \frac{\epsilon_0^2\chi^2C^2E}{\alpha(T-T_c')}\left[1-\frac{\tanh(L_c/2a)}{(L_c/2a)}\right], \quad (6)$$

where $T_c'=T_c-\frac{W_p}{\alpha}$ is the SmC^*-SmA^* transition temperature of the PSFLC system. L_c is the mean distance between two successive polymer fibers in the z direction (Fig. 13), i.e., through the thickness of the cell, and $a=\sqrt{\frac{K_2}{\alpha(T-T_c')}}$. Similarly, the average induced polarization can be written as

$$\langle P_{\rm ind}^{\rm PSFLC}\rangle = \epsilon_0\chi E + \epsilon_0\Delta\epsilon_s^{\rm PSFLC}E. \quad (7)$$

The identification between Eqs. (6) and (7) gives the expression of the dielectric strength of the soft mode, $\Delta\epsilon_s^{\rm PSFLC}$, as a function of L_c,

$$\Delta\epsilon_s^{\rm PSFLC} \approx \frac{\epsilon_0\chi^2C^2}{\alpha(T-T_c')}[1-H]. \quad (8)$$

The parameter $H=\frac{\tanh(L_c/2a)}{(L_c/2a)}$ depends on the L_c, which is directly related to the network density. For a given reduced temperature, $(T-T_c')$, Eq. (8) can be expressed as

$$\Delta\epsilon_s^{\rm PSFLC} \approx \Delta\epsilon_s^{\rm FLC}[1-H]. \quad (9)$$

$\Delta\epsilon_s^{\rm FLC}=\frac{\epsilon_0\chi^2C^2}{\alpha(T-T_c')}$ denotes the soft-mode dielectric strength of the pure FLC. Equation (9) shows that in the SmA^* phase, the main parameter that governs the soft-mode dielectric strength in the PSFLC films is L_c. This means that the stored elastic energy arising from the distortion of the director upon application of electric field becomes important when L_c is decreased. This causes a reduction in the soft-mode dielectric strength [Eq. (9)].

From Eq. (9) and the experimental data of $\Delta\epsilon_s$ [Fig. 10(a)], we evaluated the parameter L_c for each polymer concentration. To do that, the values of $\alpha\approx8.8\times10^{+3}$ N/m^2 K, $K_2\approx10^{-11}$ N, and $a=0.13$ μm [34] were used. Equation (9) was then graphically resolved to determine L_c. The results are displayed in Fig. 15. The calculated values were com-

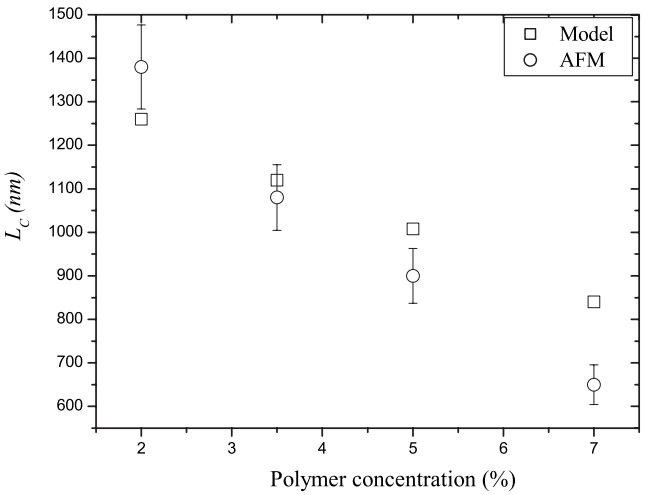

FIG. 14. The parameter L_c characterizing the network density versus polymer concentration.

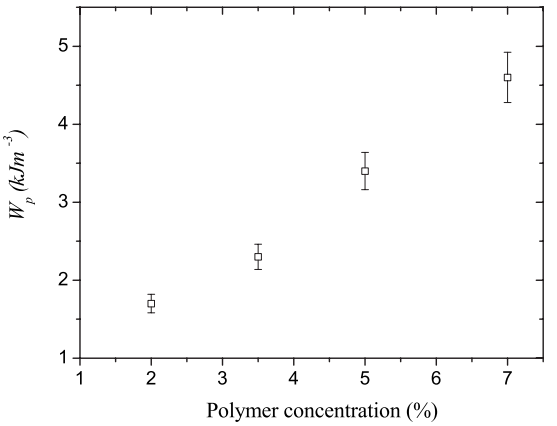

FIG. 15. The coupling parameter W_p characterizing the interaction between the FLC and the network in the SmA^* phase versus polymer concentration.

pared to those directly measured from the topography of the polymer networks obtained by means of AFM experiments (Fig. 12). It must be noted here that for AFM experiments, the PSFLC cells were disassembled and flushed with solvent to remove the FLC. Figure 12 shows example of AFM images and height profiles (on the z direction in Fig. 13) of the polymer network. The height profile in the z direction indicates two successive groups of fibers. The mean distance L_c (Fig. 12) between them was evaluated for each polymer concentration and displayed in Fig. 14. The measured values of L_c linearly decrease with the polymer density and agree well with those calculated from the model. It seems from these results that the fibrillar and anisotropic nature of the network stabilizes, at long-range scale, the SmA^* order and opposes the electric field effect on the deformation of the SmA^* director. These results are in accordance with previous works [34,35] of the electroclinic effect in the same PSFLC systems, which demonstrate that the electroclinic susceptibility of these systems is reduced with the increase in the polymer network density. It must be noted here that the average lateral separation distance (y direction in Fig. 13) between polymer strands is estimated to be about 10 μm (Fig. 12), which is 1 order of magnitude higher than L_c. This difference between interfiber distances in the two directions is an unexpected result. In fact, during the photopolymerization process, the mobility of the reactive monomers could be comparable within the smectic layers so that they present the same ability to come together and react to form the network. This ability could be significantly different across the smectic layers. Therefore, it would be reasonable to suspect that the average distance between polymer fibers could be of the same order of magnitude in lateral direction as well as in the z direction. The result found here is not yet clear, and the physical and chemical mechanisms governing the formation of the network could provide an explanation of our finding. This is not the aim of the work presented in this paper.

From the shift of the transition temperature, $\Delta T_c = T_c - T_c' = \frac{W_p}{\alpha}$, the coupling coefficient, W_p, characterizing the interaction energy between the FLC and the polymer network, can be estimated. ΔT_c values of 0.2 °C, 0.5 °C, 0.7 °C, and 0.9 °C were found for the polymer concentration of 2%, 3.5%, 5%, and 7%, respectively. The values of W_p are displayed in Fig. 15. W_p linearly increases with the polymer concentration. The linear behavior of W_p in PSFLC systems was already reported in earlier works [29,33,35]. The values of W_p found here are within 1 order of magnitude of those reported by Furue *et al.* [40], Archer and Dierking [41], and Li *et al.* [42] on other PSFLC systems.

IV. CONCLUSION

In this work, we report the influence of the polymer concentration on the collective relaxation mechanisms, namely, the soft and Goldstone modes, of a short-pitch ferroelectric liquid crystal stabilized by an anisotropic polymer network. Our studies show that the dielectric strengths of the soft and the Goldstone modes decrease with increasing polymer concentration, whereas the relaxation frequencies are shifted to high values. The reduction in $\Delta\epsilon_G$ and the increase in f_G are interpreted as a consequence of the increase in the effective twist elastic constant (K_{eff}) of the PSFLC films. The increase in the twist elasticity was related to the fibrillar structure of the polymer network. To describe the reduction in the soft-mode dielectric strength, we have adopted a one-dimensional model which takes into account both the coupling interaction between the polymer network and the liquid crystal director, and the elastic energy due to the distortion of the liquid crystal medium when an electric field is applied. The dielectric strength of the soft mode was found to be directly related to the average interfiber distance. The values of this average distance were evaluated from the model and are in agreement with those measured by atomic force microscopy.

ACKNOWLEDGMENT

This research was mainly supported by the EU Program Interreg III Intelsurf.

[1] M. Gasser, A. Gembus, D. Ganzke, and I. Dierking, Mol. Mater. **12**, 347 (2000).
[2] S. A. Rozanski, R. Stannarius, and F. Kremer, IEEE Trans. Dielectr. Electr. Insul. **8**, 488 (2001).
[3] S. A. Rozanski, R. Stannarius, F. Kremer, and S. Diele, Liq. Cryst. **28**, 1071 (2001).
[4] *Relaxation Phenomena*, edited by W. Haase and S. Wrobel (Springer, New York, 2003).
[5] H. Xu, J. K. Vij, A. Rappaport, and N. A. Clark, Phys. Rev. Lett. **79**, 249 (1997).
[6] Z. Kutnjak, S. Kralj, and S. Žumer, Phys. Rev. E **66**, 041702 (2002).
[7] S. A. Rozanski and J. Thoen, J. Non-Cryst. Solids **351**, 2802 (2005).
[8] S. A. Rozanski and J. Thoen, Liq. Cryst. **32**, 331 (2005).
[9] S. Khosla and K. K. Raina, J. Phys. Chem. Solids **65**, 1165 (2004).
[10] G. P. Crawford, R. Stannarius, and J. W. Doane, Phys. Rev. A **44**, 2558 (1991).
[11] L. Naji, F. Kremer, and R. Stannarius, Liq. Cryst. **25**, 363 (1998).
[12] D. J. Broer, R. G. Gossink, and R. A. M. Hikmet, Angew. Makromol. Chem. **183**, 45 (1990).
[13] *Liquid Crystals in Complex Geometries Formed by Polymer and Porous Networks*, edited by G. P. Crawford and S. Žumer (Taylor and Francis, London, 1996).
[14] R. A. M. Hikmet, Liq. Cryst. **9**, 405 (1991).
[15] R. A. M. Hikmet and H. M. J. Boots, Phys. Rev. E **51**, 5824 (1995).
[16] H. Shirakawa, T. Otaka, G. Piao, K. Akagi, and M. Kyotani, Synth. Met. **117**, 1 (2001).
[17] C. C. Chang, L. C. Chien, and R. B. Meyer, Phys. Rev. E **56**, 595 (1997).
[18] R. Q. Ma and D.-K. Yang, Phys. Rev. E **61**, 1567 (2000).
[19] K. Akagi, Polym. Int. **56**, 1192 (2007).
[20] M. Goh, M. Kyotani, and K. Akagi, J. Am. Chem. Soc. **129**, 8519 (2007).
[21] Y. K. Fung, D. K. Yang, Y. Sun, L. C. Chien, S. Žumer, and J. W. Doane, Liq. Cryst. **19**, 797 (1995).
[22] C. V. Rajaram, S. D. Hudston, and L. C. Chien, Chem. Mater. **8**, 2451 (1996).
[23] M. Escuti, C. C. Bowley, G. P. Crawford, and S. Žumer, Appl. Phys. Lett. **75**, 3264 (1999).
[24] I. Dierking, L. L. Kosbar, A. Afzali Ardakani, A. C. Lowe, and G. A. Held, J. Appl. Phys. **81**, 3007 (1997).
[25] G. A. Held, L. L. Kosbar, I. Dierking, A. C. Lowe, G. Grinstein, V. Lee, and R. D. Miller, Phys. Rev. Lett. **79**, 3443 (1997).
[26] K. Akagi, G. Piao, S. Kaneko, K. Sakamaki, H. Shirakawa, and M. Kyotani, Science **282**, 1683 (1998).
[27] M. Goh, T. Matsushita, M. Kyotani, and K. Akagi, Macromolecules **40**, 4762 (2007).
[28] K. Akagi, G. Piao, S. Kaneko, I. Higuchi, H. Shirakawa, and M. Kyotani, Synth. Met. **102**, 1406 (1999).
[29] M. Petit, A. Daoudi, M. Ismaili, and J. M. Buisine, Eur. Phys. J. E **20**, 327 (2006).
[30] P. J. Bos, J. A. Rahman, and J. W. Doane, SID Int. Symp. Digest Tech. Papers **24**, 877 (1993).
[31] J. Li, J. E. Anderson, C. D. Hoke, T. Nose, and P. J. Bos, Mol. Cryst. Liq. Cryst. **301**, 261 (1997).
[32] P. A. Kossyrev, J. Qi, N. V. Priezjev, R. A. Pelcovits, and G. P. Crawford, Appl. Phys. Lett. **81**, 2986 (2002).
[33] I. Dierking, M. A. Osipov, and S. T. Lagerwall, Eur. Phys. J. E **2**, 303 (2000).
[34] M. Petit, A. Daoudi, M. Ismaili, and J. M. Buisine, Phys. Rev. E **74**, 061707 (2006).
[35] M. Petit, A. Daoudi, M. Ismaili, J. M. Buisine, and A. Da Costa, Mol. Cryst. Liq. Cryst. Suppl. Ser. **487**, 61 (2008).
[36] T. Carlsson, B. Zeks, C. Filipic, and A. Levstik, Phys. Rev. A **42**, 877 (1990).
[37] M. Brunet, J. Phys. Colloq. **36**, C1 (1975).
[38] S. Kundu, T. Ray, S. K. Roy, W. Haase, and R. Dabrowski, Ferroelectrics **282**, 239 (2003).
[39] E. Beckel, N. B. Cramer, A. W. Harant, and C. N. Bowman, Liq. Cryst. **30**, 1343 (2003).
[40] H. Furue, T. Takahashi, and S. Kobayashi, Jpn. J. Appl. Phys., Part 1 **38**, 5660 (1999).
[41] P. Archer and I. Dierking, J. Phys. D **41**, 155422 (2008).
[42] J. Li, X. Zhu, L. Xuan, and X. Huang, Ferroelectrics **277**, 85 (2002).